ELSEVIER

FEMS Microbiology Ecology 46 (2003) 247–255

FEMS MICROBIOLOGY Ecology

www.fems-microbiology.org

The role of aggregation for the dissolution of diatom frustules

Uta Passow [a,*], Anja Engel [a], Helle Ploug [b]

[a] *Alfred-Wegener-Institut für Polar und Meeresforschung, Bremerhaven, Germany*
[b] *Max-Planck Institut für Marine Mikrobiologie, Bremen, Germany*

Received 15 November 2002; received in revised form 26 June 2003; accepted 7 July 2003

First published online 27 August 2003

Abstract

Observations that the majority of silica dissolution occurs within the upper 200 m of the ocean, and that sedimentation rates of diatom frustules generally do not decrease significantly with depth, suggested reduced dissolution rates of diatoms embedded within sinking aggregates. To investigate this hypothesis, silica dissolution rates of aggregated diatom cells were compared to those of dispersed cells during conditions mimicking sedimentation below the euphotic zone. Changes in the concentrations of biogenic silica, silicic acid, cell numbers, chlorophyll *a* and transparent exopolymer particles (TEP) were monitored within aggregates and in the surrounding seawater (SSW) during two 42-day experiments. Whereas the concentration of dispersed diatoms decreased over the course of the experiment, the amount of aggregated cells remained roughly constant after an initial increase. Initially only 6% of cells were aggregated and at the end of the experiment more than 60% of cells were enclosed within aggregates. These data imply lower dissolution rates for aggregated cells. However, fluxes of silica between the different pools could not be constrained reliably enough to unequivocally prove reduced dissolution for aggregated cells.
© 2003 Federation of European Microbiological Societies. Published by Elsevier B.V. All rights reserved.

Keywords: Diatom frustule; Silica dissolution; Aggregation

1. Introduction

The rate of silica dissolution from diatom frustules determines the fraction of silica recycled within the euphotic zone where it is available for new growth, as well as the fraction of biogenic silica which is recycled at depth or buried forming diatomaceous ooze. Even though the solubility of biogenic silica ($BSiO_2$) in seawater is very high, >1000 μM at 15°C [1] and the ocean is undersaturated in silicic acid (upper ocean: 0–50 μM, deep ocean: <180 μM [2]), dissolution rates of diatom frustules are generally low. Diatom frustules are protected from immediate dissolution by an organic coating consisting of three layers, a polysaccharide, a lipid and a protein layer [3]. High dissolution rates of diatom frustules occur when bacterial degradation removes this protective organic matrix [4,5].

Diatoms settle to the deep ocean predominantly as aggregates [6]. Measurements within aggregates indicate that the microenvironment of aggregates differs considerably from environmental conditions in the surrounding water [7–10]. Consequently, the rate of biological and chemical processes within aggregates may differ fundamentally from those in the surrounding seawater (SSW). Dissolution rates of diatom frustules, for example, may be reduced or elevated within aggregates compared to those of freely suspended cells. High bacterial activity within aggregates may increase average dissolution rates due to the removal of the protective organic matrix. However, if the exchange rate between the pore water of aggregates and the SSW is low, the accumulation of silicic acid within aggregates may decrease dissolution rates of diatom frustules, because once the organic coating is removed, dissolution rate is a function of the concentration gradient between frustules and the adjacent water. Preliminary experimental evidence suggested relatively low dissolution rates (1.6% day^{-1}) when phytodetritus was aggregated compared to non-aggregated material [11], but a different study did not observe differences in dissolution between clumped and free cells [4]. Dissolution rates of frustules within intact fecal pellets are reduced [12], suggesting that frustules packed in marine snow may also be protected from dissolution. A

* Corresponding author. Tel.: +49 (471) 4831 1450; Fax: +49 (471) 4831 1425.
E-mail address: upassow@awi-bremerhaven.de (U. Passow).

0168-6496/03/$22.00 © 2003 Federation of European Microbiological Societies. Published by Elsevier B.V. All rights reserved.
doi:10.1016/S0168-6496(03)00199-5

Downloaded from https://academic.oup.com/femsec/article/46/3/247/520432 by Max-Planck-Institute Bremen user on 15 December 2020

minimal decrease in sedimentation rates of diatoms with depth, also imply that dissolution of frustules is insignificant during marine snow-mediated sinking [13].

In this study we investigated the dissolution of diatom cells during conditions mimicking their sedimentation as aggregated or dispersed cells. We hypothesized that the average dissolution rates of aggregated cells would be appreciably lower than that of freely suspended cells. Specifically, we monitored silica dissolution of the diatom *Thalassiosira weissflogii*, sampling aggregated and freely dispersed cells separately. Concentrations of bacteria and transparent exopolymer particles (TEP) were also monitored during the experiments.

2. Materials and methods

2.1. Experimental approach and set-up

The experiments were set-up to compare silica dissolution of living *T. weissflogii* cells within aggregates with those of dispersed cells in the SSW during conditions imitating continuous sinking in the dark (Fig. 1). A multi-bottle approach, where replicate bottles were sacrificed at each time point, was chosen, as it is nearly impossible to subsample from a population of aggregates, because of their high variability (e.g. cell numbers of different aggregates of similar size may vary widely). Aggregated and dispersed cells were incubated together and separated prior to analysis rather than before incubation, to guarantee identical start-up conditions in each bottle. A separation of aggregates and dispersed cells before incubation is precarious, because aggregates easily break or get damaged during handling and because it is impossible to prepare enough aggregates of the same size and cell concentration to generate a set of replicate bottles of aggregates.

Before the experiment, the solitary, centric central diatom *T. weissflogii* was grown in two batch cultures at 15°C with a light flux of 100 μmol m^{-2} s^{-1} in a 12 h:12 h light:dark cycle. F/2 media based on seawater was used [14], except that nutrient concentrations were reduced to 30% to avoid artificially high cell concentrations. Nutrient concentrations were kept non-limiting in one culture, whereas silicic acid concentration was run to depletion in the second culture to ensure a low background concentration of silicic acid at the start of the experiment. Two identical experiments, experiments A and B, were conducted. Both experiments were designed to last for 42 days with nine sampling days spread evenly over the incubation period. Because three replicate bottles were to be sacrificed on each sampling day, a total of 27 gas-permeable bottles (LDPE, Nalgene) with a volume of 116 ml each were prepared at the beginning of each experiment. Each bottle was filled with a mixture of growing diatoms from the first culture (nitrate: 184 μM, phosphate: 2.4 μM, silicic acid: 9.6 μM) and diatom-free filtrate generated from the second culture (nitrate: 185 μM, phosphate: 2.9 μM, silicic acid: 0.7 μM) to achieve an end concentration of about 3000 cells ml^{-1}. Each bottle was filled bubble-free, by closing the bottle while submerged. Bottles

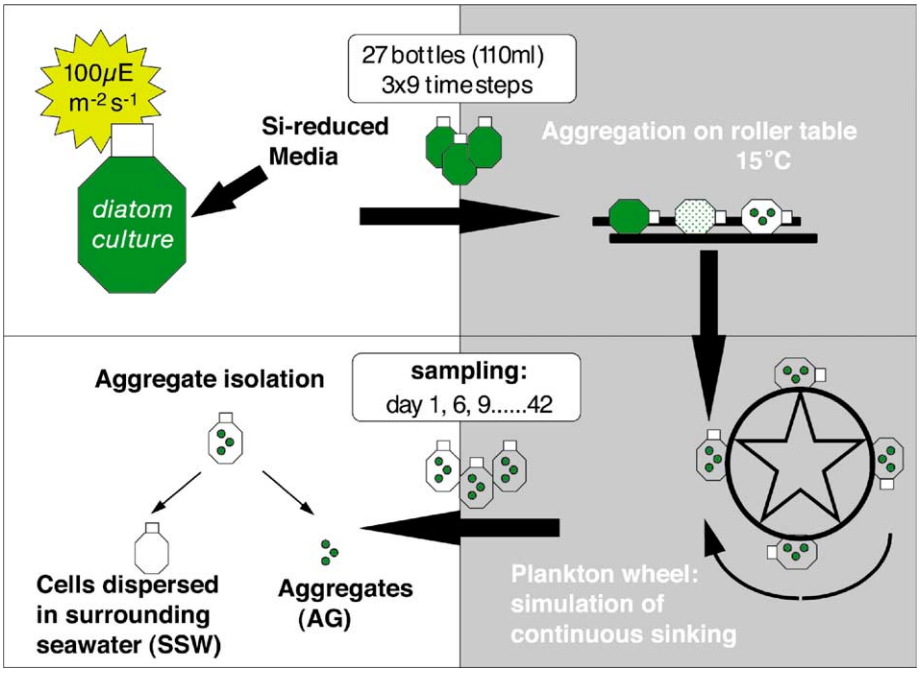

Fig. 1. Experimental set-up: Two identical experiments lasting 42 days were conducted in the dark. Diatoms grown in silicic acid reduced media were initially incubated on a rolling table for 48 h to promote aggregate formation and then incubated on a plankton (Ferris) wheel to simulate continuous sinking. At each sampling date three replicate bottles were removed and the aggregates separated from the SSW. Both fractions were then analyzed separately.

Downloaded from https://academic.oup.com/femsec/article/46/3/247/520432 by Max-Planck-Institute Bremen user on 15 December 2020

and lids were handled with sterilized tongs while submerged in the diatom suspension. Bubbles would create turbulence and shear in bottles rotating on a Ferris wheel, increasing collisions between cells, aggregates and bottle walls, rather than mimicking sinking. The experiments were conducted in the dark at a temperature of 15°C. During the first 48 h bottles were incubated on a roller table to promote aggregation [15]. When aggregates were visible, the bottles were transferred carefully to a Ferris wheel (diameter = 0.9 m) and rotated continuously end over end at about 1 rpm to simulate continuous sinking in a low-shear environment.

Visible aggregates (≥ 1 mm) and the SSW without visible aggregates were analyzed separately. On each sampling day, aggregates were isolated with a 10 ml syringe equipped with a 1 mm diameter needle. The total volume of the aggregate slurry for each bottle was recorded to the nearest 0.1 ml, and 35‰ NaCl solution was added to bring the total volume to 100 ml. The remaining volume of SSW was also documented for each bottle.

2.2. Analysis

On each sampling day, subsamples for the determination of the following variables were taken from both fractions (the aggregate slurry and the SSW fraction) of each of three replicate bottles. Nutrients (NO_3, PO_4 and $Si(OH)_4$) were analyzed with an autoanalyzer [16]. Biogenic silica was measured from 50–60 ml sample filtered onto 0.4 μm polycarbonate filters and analyzed according to Koroleff [16]. Chlorophyll *a* was determined in a Turner fluorometer [17] from two replicate GF/F filters onto which 4–8 ml of sample were filtered. Phytoplankton abundance was determined from 20 ml samples, which were preserved with 4 ml of formalin (20%). Phytoplankton cells were counted using an inverted microscope (Zeiss) at magnifications of 250× and 400×. TEP were analyzed colorimetrically from 20 ml [18] and microscopically from 10 ml filtered onto 0.4 μm membrane filters (Poretics) with two replicates each [19]. Two replicate black 0.2 μm membrane filters (Poretics) were prepared from 2–4 ml sample, fixed with 0.2 μm pre-filtered formalin (40%) and stained with 0.5 ml of pre-filtered (0.2 μm) 4,6-diamino-2-phenylindole (DAPI) for the enumeration of bacteria. Stained filters were mounted onto glass slides, covered with immersion oil and a glass cover and frozen at −20°C. Slides were then transferred to a fluorescent light microscope (Zeiss, 340 nm light source) and screened by a Panasonic color video camera on Super VHS at a magnification of 1000×. Fifty frames were chosen in a cross-section and digitized on a Macintosh PPC with an optical resolution of 0.028 μm^2 per pixel. Bacteria were enumerated and sized semi-automatically by the image analysis program NIH-Image 6.1 ppc, a public domain program developed at the US National Institute of Health.

Whereas it was straightforward to calculate the concentrations of the particulate and dissolved constituents in the SSW, as well as the concentrations of particulates enclosed within aggregates from measured amounts and volumes, calculations of the concentrations of solutes in the pore water of aggregates are prone to high errors. The determination of the pore water volume necessitates a set of assumptions regarding the porosity [20–22] and fractal nature of aggregates [23–26], the size of the boundary layer and plume of aggregates [9,27,28], the flow fields around or through aggregates [20,29] and the molecular diffusion coefficient of silicic acid out of aggregates [10]. Past estimates of nutrient concentrations in pore water of aggregates may be too high, if they are based on calculations ignoring the newly hypothesized plume surrounding aggregates. The volume of water characterized by elevated concentrations includes both the pore water of the aggregate and the water in the plume. Several of the estimates needed to calculate pore water concentrations are currently not well constrained and discussed very controversially. Here we thus only present the data of solutes in pore water as absolute amounts, not concentrations.

3. Results and discussion

We analyzed data of both experiments, but because initial concentrations of dissolved and particulate matter were not significantly different and because all results of

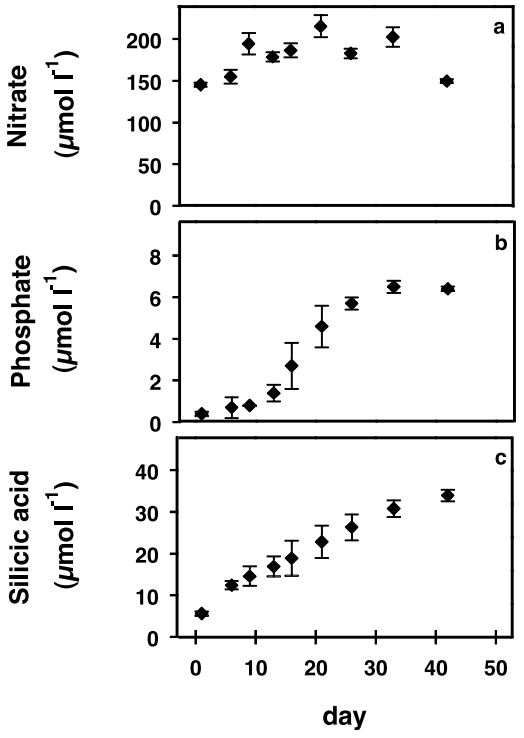

Fig. 2. Overall development of nutrient ((a) nitrate, (b) phosphate and (c) silicic acid) concentrations in bottles (aggregate and SSW fractions combined) during experiment A. Averages and standard deviation of the three replicate bottles are depicted.

Downloaded from https://academic.oup.com/femsec/article/46/3/247/520432 by Max-Planck-Institute Bremen user on 15 December 2020

experiments A and B showed the same trend, only data from experiment A are presented.

3.1. General development of dissolved and particulate constituents

To sketch the overall development during the experiment, averages of the total concentrations of nutrients (Fig. 2) and particles (Fig. 3) are depicted from the three replicate bottles during the 42-day period. Nitrate concentration was high throughout and increased slightly during the first 20 days of the experiment (Fig. 2a). Initially, phosphate concentration was low (0.4 μM) and after a lag period of 12 days, increased exponentially to a final value of 6.4 μM (Fig. 2b). At the beginning of the experiment, the concentration of silicic acid was low (5.6 μM), but increased linearly from the beginning of the experiment to 34 μM indicating rapid dissolution of biogenic silica from the start (Fig. 2c).

In contrast to chlorophyll *a*, which began decreasing during the first days of the study, the diatom abundance remained constant during the first 2 weeks but decreased by roughly two thirds thereafter (Fig. 3a,b). Biogenic silica began decreasing without delay (Fig. 3d), mirroring the

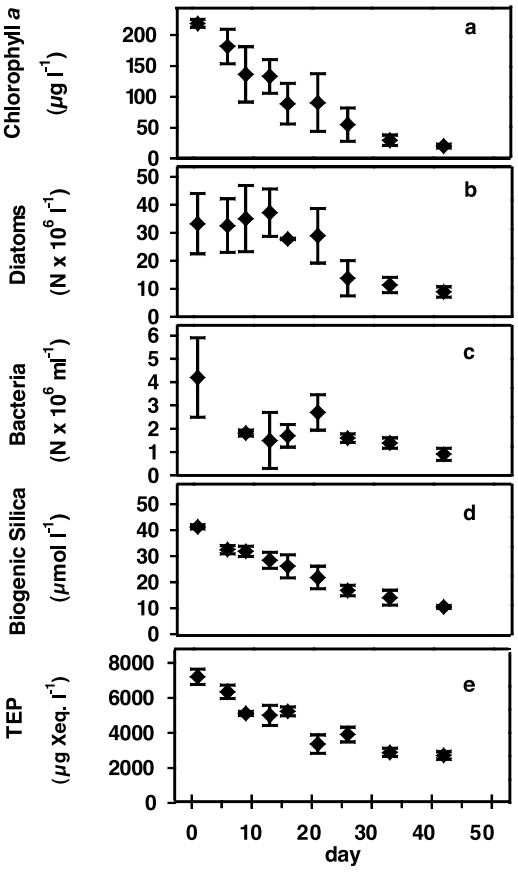

Fig. 3. Overall development of the (a) chlorophyll *a*, (b) diatoms, (c) bacteria, (d) BSi and (e) TEP concentrations in bottles (aggregate and SSW fractions combined) during experiment A. Averages and standard deviation of the three replicate bottles are depicted.

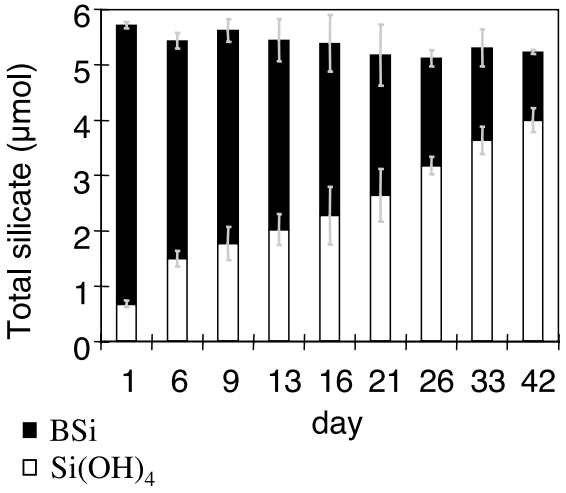

Fig. 4. Overall development of dissolved and biogenic silica concentrations in bottles (aggregate and SSW fractions combined) during experiment A. Averages and standard deviation of the three replicate bottles are given. Note the non-linear timescale.

increase in silicic acid concentration (Fig. 4). The total flux of silica from the biogenic into the dissolved pool was equal to 5 μmol per bottle during the 42-day experiment. Whereas dissolution of silica frustules and the decline of chlorophyll *a* began within 1 or 2 days after the onset of darkness, the loss of cells and the degradation of phosphor were delayed for almost 2 weeks after the onset of darkness, suggesting a temporal decoupling between the degradation of cells and silica dissolution.

Initial concentrations of TEP were high (8000 μg xanthan equivalent l^{-1}) and decreased by one half during the first 20 days of the experiment, but remained almost constant thereafter (Fig. 3e). TEP are a chemically heterogeneous group of particles and whereas one fraction was degraded on timescales of days, degradation of the remaining fraction may have been appreciably lower. Alternatively enhanced production of TEP by bacteria may have compensated loss by degradation during the second half of the experiment. Total bacterial concentration initially decreased and then fluctuated around 2×10^9 cells l^{-1} with a slight decreasing tendency (Fig. 3c).

3.2. Developments of dissolved and particulate constituents within the different compartments

The dynamics of diatom and bacteria numbers, as well as of chlorophyll *a*, biogenic silica and TEP concentrations in the SSW fraction reflected predominantly the decrease observed in the SSW plus aggregate fraction presented above, except that the decreases were more pronounced in the SSW fractions compared to the combined fractions.

The amount of chlorophyll *a*, biogenic silica, diatoms and TEP collected in the aggregate slurry increased during the first 2 weeks of the study (Fig. 5). During the following 10 days, variability between replicate bottles was high, but

Downloaded from https://academic.oup.com/femsec/article/46/3/247/520432 by Max-Planck-Institute Bremen user on 15 December 2020

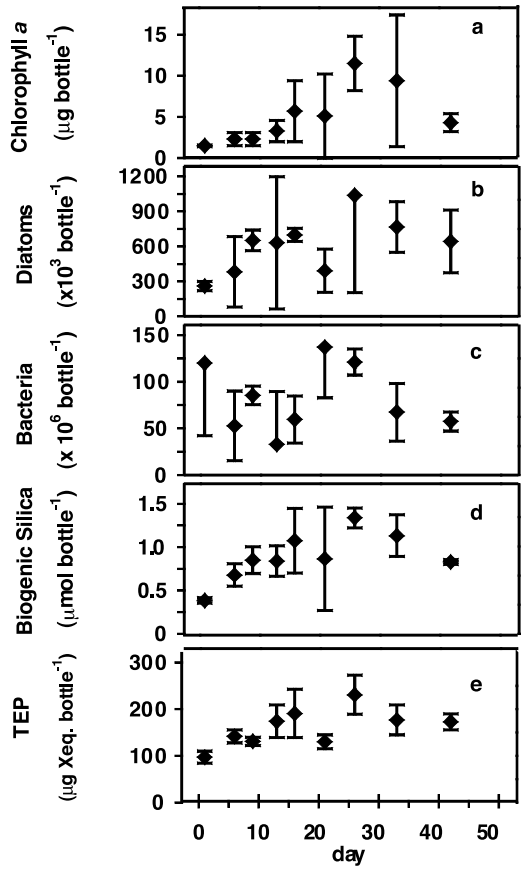

Fig. 5. Overall development of the amount of (a) chlorophyll *a*, (b) diatoms, (c) bacteria, (d) BSi and (e) TEP and sampled in aggregate slurries during experiment A. Averages and standard deviation of the three replicate bottles are depicted.

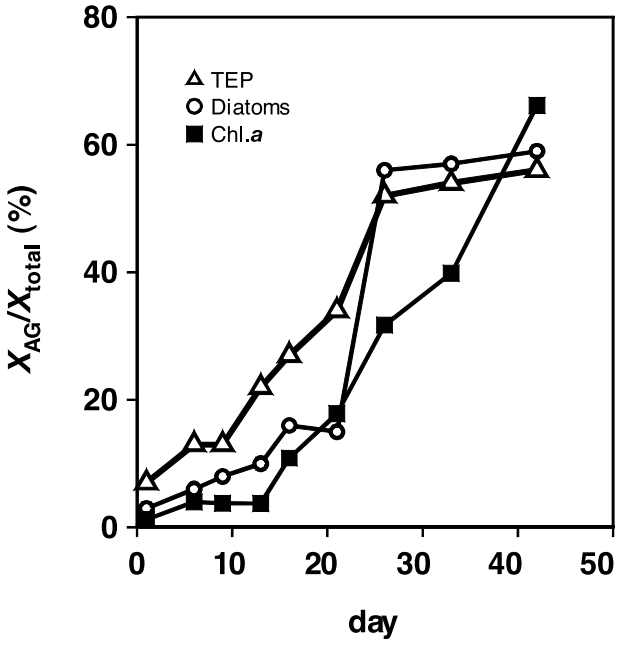

Fig. 6. Percentage of total amount of chlorophyll *a* (filled squares), TEP (open triangles) and diatoms (open circles) contained in aggregates during experiment A.

no net change was visible. After day 25 the concentrations of chlorophyll *a*, biogenic silica, cell number and TEP in the aggregate slurry were high, but decreased during the remainder of the study. Less than 20% of TEP or diatoms were incorporated in the visible aggregates before the period of high variability, but after day 25 more than 50% of these particles were sampled in the aggregate slurry (Fig. 6). No net change in bacterial numbers within aggregate slurries was observed during the initial 15 days (Fig. 5c). Bacteria concentrations within aggregates ($2.2 \pm 1.0 \times 10^7$ cells ml^{-1}) were low and on average only one order of magnitude higher than in the SSW, where abundance was comparable to natural seawater with $1.2 \pm 3.7 \times 10^6$ cells ml^{-1}.

Qualitatively, the aggregated material did not differ in a statistically significant way (*t*-test, $\alpha = 0.05$) from the freely suspended material, as indicated by the ratios between chlorophyll *a*, biogenic silica or TEP and cell numbers, with one exception. During the initial 15 days of the experiment the chlorophyll *a* concentration per cell was significantly lower in aggregated compared to free material, suggesting either preferential loss of chlorophyll *a* within aggregates or preferential aggregation of chlorophyll *a*-poor cells. On each day, the biogenic silica content per cell was higher in aggregated cells compared to free cells, but overall this difference between aggregated and free cells was not statistically significant, because of the high day-to-day variability. The ratio between bacteria and diatoms increased in SSW and fluctuated without trend in aggregates, but the average ratio was similar in both fractions.

3.3. Flux of silica between the different pools

Silica was measured in all four compartments; as biogenic (particulate) silica in the SSW and in aggregates and as silicic acid both in the SSW and within pore water of aggregates. The net decrease of biogenic silica in the SSW

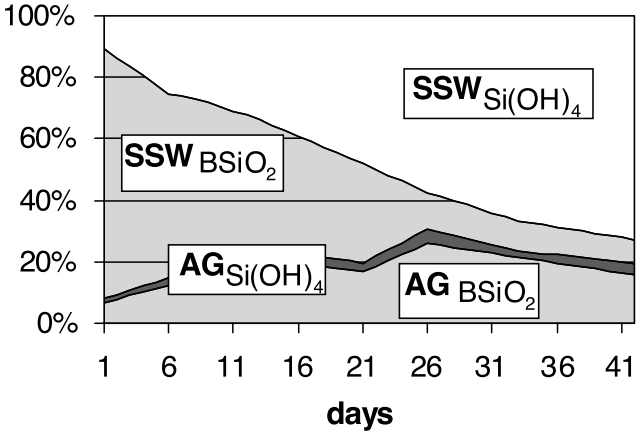

Fig. 7. Silica budget, showing the contributions of the biogenic silica in aggregates (AG_{BSIO2}), and the SSW (SSW_{BSIO2}) as well as the silicic acid content in aggregates ($AG_{Si(OH)4}$) and the SSW ($SSW_{Si(OH)4}$).

Downloaded from https://academic.oup.com/femsec/article/46/3/247/520432 by Max-Planck-Institute Bremen user on 15 December 2020

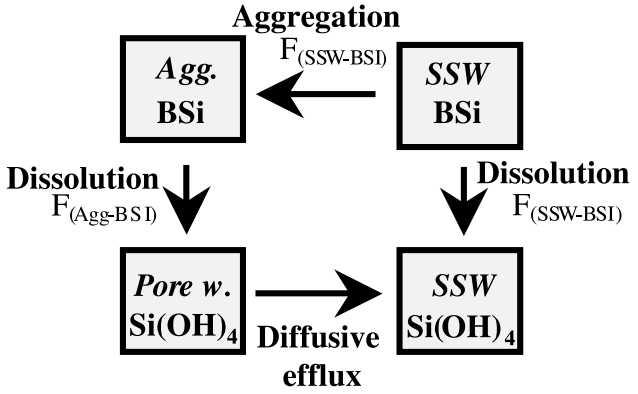

Fig. 8. Simple box model depicting the four silica pools and the major fluxes between these pools. Agg. BSi, biogenic silica in aggregated particles; SSW BSi, biogenic silica of particles in the SSW; pore w. $Si(OH)_4$, silicic acid in pore water of aggregates; SSW $Si(OH)_4$, silicic acid in the SSW.

was compensated by a net increase of silicic acid in the SSW and a smaller net increase in biogenic silica in aggregates (except during the last day) (Fig. 7). As the total amount of silicic acid in the pore water was small, the change in the silicic acid amount in the pore water was also very small. It is assumed that the formation of biogenic silica due to growth was negligible during the study, as the experiments were conducted in the dark. Diatom uptake of silicic acid can continue for only a few hours to a day in the dark [30]. Net disaggregation was also assumed to be negligible, as aggregates appeared sturdy and did not break even during handling. Aggregation and dissolution of cells as well as the efflux of solutes out of aggregates are thus the major potential mechanisms responsible for the flux of silica between the four pools (Fig. 8).

3.3.1. Dissolution

Concentrations of silicic acid within the dispersed cell fraction initially were 5 μM and increased to 33 μM at the end, covering a range well comparable to natural seawater and far below saturation concentrations which are >1000 μM [1,31]. Within the range covered during our experiment the overall dissolution rate of aggregated plus dispersed cells was constant ($r^2 = 0.97$) at 0.079 μmol per day per bottle, indicating that dissolution during our experiment was independent of the biogenic silica concentration. If the experiment were continued further, dissolution rate would decrease as the biogenic silica concentration decreased. In the past, different models have been used to represent the kinetics of biogenic silica dissolution, depending on assumptions regarding the dissolution mechanism [32]. As silica dissolution remained in the linear section of the dissolution curve during our experiment (meaning it was independent of biogenic silica concentration), dynamics of silica dissolution could be fitted using any of several models describing silica dissolution (for an overview of models see [32]). The simplest model, the Nernst diffusion approach assumes that dissolution is limited by the rate of diffusion through a boundary layer ($r^2 = 0.97$, $df = 7$). The surface reaction approach assumes that dissolution is limited by surface chemistry, rather than diffusion ($r^2 = 0.97$, $df = 7$). The parabolic law approach assumes that the reaction rate is limited by diffusion, differentiating between each dissolved species ($r^2 = 0.99$, $df = 7$) and the decreasing surface approach additionally assumes a decreasing surface area as dissolution progresses ($r^2 = 0.94$, $df = 25$).

Daily specific dissolution rates of aggregated plus dispersed cells normalized by the initial concentration of BSi decreased from 3.3 to 1.7% day^{-1} (0.033 to 0.017 cells dissolved day^{-1}), with a linear average of $2.3 \pm 0.5\%$ day^{-1} (0.023 ± 0.005 cells dissolved day^{-1}) or a value of 2.6% day^{-1} (0.026 cells dissolved day^{-1}) calculated from an exponential curve fit using the initial concentration of biogenic silica as a potential maximum (Fig. 9). More than 60% of biogenic silica dissolved during the 42-day experiment (Fig. 9). A dissolution rate of 40–70% of diatom frustules in 40–50 days was also found for several other diatom species, independent whether cells were alive or heat killed, whether they were fragmented or intact, as long as bacteria were present [4]. The main factor determining the dissolution rate of diatom frustules is the presence or absence of bacteria [4,5]. Dissolution rates in the absence of bacteria were found to be 2–20 times lower. Bacteria-mediated specific dissolution rates of fresh phytodetritus of *T. weissflogii* ranged between 2.1 and 7.9% day^{-1} initially and between 2.0 and 3.2% day^{-1} between day 2 and 10 depending on the colonizing bacteria [5]. Contrary to this latter study no initial increase in bacterial

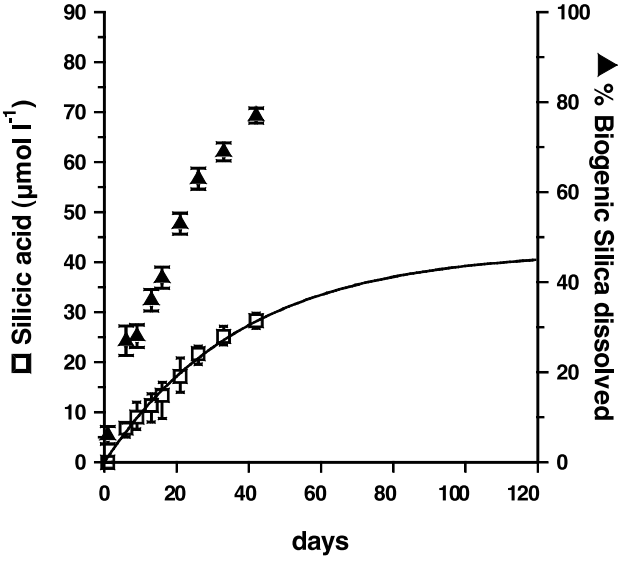

Fig. 9. Dissolution dynamics of diatom frustules depicted as the increase in silicic acid concentration and as the % of biogenic silica solubilized. Data points and standard deviations between replicate bottles are given. Changes in the silicic acid dissolution fit the curve: Silicic acid = $42.36 (1-e^{-0.026*t})$, $r^2 = 0.99$, $df = 8$.

Downloaded from https://academic.oup.com/femsec/article/46/3/247/520432 by Max-Planck-Institute Bremen user on 15 December 2020

numbers was observed in our study. Moreover, concentrations of bacteria in aggregates were low during our study compared to the much higher enrichment of bacteria often found in aggregates; see compilation of data in [33].

A net decrease in biogenic silica was observed in SSW only, no net decrease of cells was observed in the aggregate slurry fraction, and after an initial increase the amount of silicic acid in pore water remained roughly constant, implying that no significant net dissolution occurred. Assuming that no exchange between the aggregated and the dispersed cell fractions took place, the dissolution rate in SSW was 0.65 μmol l^{-1} day^{-1} (linear, $r^2 = 0.97$) and the specific dissolution rate normalized to daily biogenic silica concentrations increased during the experiment by an order of magnitude from 0.017 to 0.18 day^{-1} due to the decreasing biogenic silica concentration. In aggregates the dissolution rate was 0.01 μmol l^{-1} day^{-1} (highly variable, no significant relationship) with a specific dissolution rate ranging from 0.001 to 0.003 day^{-1}, again assuming that no exchange between the aggregated and the dispersed cell fractions took place. Possibly silicic acid concentration in pore water was high enough to inhibit dissolution of aggregated cells. Or, diatom frustules within aggregates were protected chemically (by organic substances) reducing dissolution. Alternatively, dissolution of aggregated cells was higher than estimated above, but balanced by continuous aggregation. This scenario is supported by the fact that the overall specific dissolution rate didn't decrease appreciably after 26 days, although 60% of all diatoms were imbedded in aggregates from that day on. In this scenario, the concomitant production of silicic acid would have to be balanced by its efflux out of aggregates.

3.3.2. Aggregation

After the initial increase in the concentrations of diatoms in the aggregate slurry fraction during the first 15 days of the experiment, no net changes were observed, indicating that no further aggregation occurred or that the increase of particles in aggregates due to aggregation was balanced by dissolution. Using a simple coagulation model we estimated a maximal aggregation rate to evaluate if the decrease in freely suspended cells during the experiment could theoretically be explained by their inclusion in aggregates, rather than by their dissolution. Initial calculations had suggested that the flux from the dispersed fraction into the aggregate fraction was dominated by scavenging of dispersed cells by aggregates due to differential settling, whereas aggregation of single cells with each other due to shear was comparably small. Assuming maximum aggregation, e.g. that cells were lost from the SSW by aggregation only, we calculated the maximal transfer of cells into the aggregates using the basic coagulation equations given by Jackson [34] under the assumption of two size classes; single cells and large, visible aggregates:

$$C_{1,2} = \alpha * N_1 * N_2 * \{[\pi/4 * (d_1 + d_2)^2 * (|w_1 - w_2|)] + [G/6 * (d_1 + d_2)^3]\}$$

where $C_{1,2}$ is the coagulation rate (m^{-3} s^{-1}), α the attachment probability, G the shear rate (s^{-1}) and N_1, N_2 (m^{-3}), d_1, d_2 (m) and w_1, w_2 (m s^{-1}) the particle concentrations, diameters and sinking velocities, respectively, in the two size classes. From initial experimental conditions we set $G = 0.2$ s^{-1}; N_1 and N_2 5×10^6 cells m^{-3} and 10 aggregates m^{-3}, respectively; d_1 and d_2 0.00001 and 0.002 m, respectively; and estimated w_1 and w_2 from size as 0.5 and 50 m day^{-1} according to Alldredge and Gotschalk [21].

Results of this simple model suggest that the observed decrease in the concentration of dispersed cells could be explained by aggregation due to scavenging of individual cells by large aggregates. The stickiness coefficient necessary to explain observations assuming all cells lost from SSW aggregated was $\alpha = 0.004$. This is considered a low value in the presence of high TEP concentrations [35,36] and clearly reasonable.

3.3.3. Diffusive efflux

As both biogenic silica and silicic acid concentrations in aggregates remained largely unchanged (within our ability to measure these), possible aggregation and subsequent dissolution of cells in aggregates must have been balanced by loss due to diffusion of silicic acid out of aggregates. Alternatively, all dissolution occurred in the SSW rather than in aggregates, implying that both, the influx of biogenic silica due to aggregation and the efflux of silicic acid out of aggregates were negligible.

Estimates of advective or diffusive loss of solutes from marine snow differ widely. Because marine aggregates have porosities > 0.99 (e.g. their solid volume is small), and because neither their sinking velocity nor their coagulation rates with smaller particles can be predicted assuming solid spheres [37–39], it has been argued that advective and diffusive exchange of solutes between aggregates and the surrounding water may be large (e.g. [20]). A large fraction of the non-solid volume of aggregates, however, is filled with a polysaccharide matrix [40,41], and especially diatom aggregates contain large amounts of mucus, which consists of TEP [42,43]. The volume fraction of aggregates, which is filled by such a mucus matrix, and its impact on the efflux of solutes are largely unknown. Possibly this polymer network of the mucus matrix traps the interstitial water, thus effectively reducing advective exchange of solutes between aggregates and the SSW. Both, the fractal nature of aggregates [23] and this mucus matrix of aggregates could physically reduce the efflux of solutes out of aggregates.

Experimental studies have shown that total oxygen exchange between sinking aggregates and the surrounding water could largely be explained by diffusion as the sole mass transfer process within aggregates similar to those of

Downloaded from https://academic.oup.com/femsec/article/46/3/247/520432 by Max-Planck-Institute Bremen user on 15 December 2020

the present study (Ploug et al., 2002). Aggregate volumes are in the order of μl. Direct measurements of concentrations and, hence, diffusion coefficients of solutes within aggregates are therefore difficult. An estimate based on point measurements of the concentration gradients of oxygen using oxygen microsensors within and around aggregates yielded a diffusion coefficient of oxygen within aggregates near that expected in stagnant seawater [9]. Other experiments adding tetrazolium salts to SSW, however, suggested that diffusion rates were greatly reduced compared to diffusion in stagnant seawater as the reaction with tetrazolium salts within aggregates appeared slow [7]. A diffusion coefficient for silicic acid out of natural marine snow, estimated to be at least 20–200 times less than that predicted by molecular diffusion in seawater, was derived from a budget of the silica cycle within aggregates, but no time series data were available [10]. More advanced tools like nuclear magnetic resonance imaging and diffusivity microsensors with high spatial resolution as used in sediments have not yet been used for more direct measurements of diffusivity in diatom aggregates and marine snow [44,45].

3.4. Evaluation of the experiment on the dissolution of aggregated and dispersed diatom frustules

The experiment was conducted to look at dissolution of diatom frustules while they settle to depth. Incubation conditions mimicked sinking in the dark, deep ocean. Bottles were transparent for gas allowing oxygen and carbon dioxide to remain at reasonable levels. Conditions inside bottles did not deteriorate (in contrast of batch cultures at senescence). Although wall effects can't be excluded, none were observed and bacterial concentration remained realistic, even low. Live phytoplankton cells were still observed after 42 days of the experiment. The exclusion of grazers was a prerequisite for comparing dissolution rate of aggregated and dispersed cells. Dissolution rates of grazed frustules need to be assessed for evaluation of silica dissolution in the ocean, but were beyond the scope of this paper.

Although results appear to show that dissolution of aggregated diatom frustules was appreciably slower than that of dispersed cells, aggregation dynamics were so complex that the possibility that aggregation compensated for loss of aggregated cells due to dissolution could not be excluded. The exchange rate of silicic acid between pore water and the SSW is also too uncertain to constrain flux of silica between aggregates and SSW. Assuming a diffusion coefficient of silicic acid within aggregates to be similar to molecular diffusion in stagnant seawater, the aggregation rate and the subsequent efflux of silicic acid out of aggregates could have been high enough to generate observed patterns, even if dissolution rates in aggregates were higher than those of freely suspended cells. In other words, although the enrichment of cells in aggregates at the conclusion of the experiment suggests a higher dissolution rate for freely suspended cells, the data of this experiment can not exclude the possibility that dissolution rate of dispersed cells was similar or even higher than that of aggregated cells. In a future experiment aggregated and dispersed cells will have to be separated a priori.

3.5. Significance for field observations

Observations suggest that most of the dissolution of biogenic silica is confined to a few hundred meters from the sea surface. The observed decrease in flux of biogenic silica to depth is comparatively low [13,46–48]. High dissolution rates of diatom frustules observed in the upper layer of the ocean have been explained by bacteria-mediated dissolution of unaggregated cells [4,5]. Within the euphotic zone, average dissolution rates of aggregated cells are similar [10], as high primary production [8] and high uptake rates of silicic acid by some of the aggregated cells are compensated by high dissolution rates of others [10]. We had hypothesized that low dissolution rates within aggregates could explain reduced dissolution rates below the mixed layer, because diatoms reach greater depth only via aggregates or within fecal pellets. Alternatively, the decline in silica dissolution rates with depth may be explained by aggregation and subsequent rapid sedimentation of cells. Changes in the average sinking velocity of diatoms due to their inclusion in fast sinking aggregates rather than differences in dissolution rates would also result in decreased recycling of silica at depth.

Acknowledgements

We thank Rolf Peinert, Peter Fritsche, Ursula Junghans, Kerstin Nachtigall, Dorothee Adams, Jenny Dannheim and Gabi Donner for help with the sampling and Geoff Evans, Mark Brzezinski, Kumiko Azetsu-Scott, Bruce Logan and Dieter Wolf-Gladrow for discussions. This research was funded by the Deutsche Forschungsgemeinschaft and the Alexander von Humboldt Foundation.

References

[1] Cappellen, P.V. and Qui, L. (1997) Biogenic silica dissolution in sediments of the Southern Ocean: I Solubility. Deep-Sea Res. II 44, 1109–1128.
[2] Treguer, P. et al. (1995) The Silica balance in the world ocean: A reestimate. Science 268, 375–379.
[3] Hecky, R.E. et al. (1973) The amino acid and sugar composition of diatom cell walls. Mar. Biol. 19, 323–331.
[4] Patrick, S. and Holding, A.J. (1985) The effect of bacteria on the solubilization of silica in diatom frustules. J. Appl. Bacteriol. 59, 7–16.
[5] Bidle, K.D. and Azam, F. (1999) Accelerated dissolution of diatom silica by marine bacterial assemblages. Nature (London) 397, 508–512.

Downloaded from https://academic.oup.com/femsec/article/46/3/247/520432 by Max-Planck-Institute Bremen user on 15 December 2020

[6] Alldredge, A.L. and Gotschalk, C.C. (1989) Direct observations of the mass flocculation of diatom blooms: Characteristics, settling velocities and formation of diatom aggregates. Deep-Sea Res. 36, 159–171.
[7] Shanks, A.L. and Reeder, M.L. (1993) Reducing microzones and sulfide production in marine snow. Mar. Ecol. Prog. Ser. 96, 43–47.
[8] Gotschalk, C.C. and Alldredge, A.L. (1989) Enhanced primary production and nutrient regeneration within aggregated marine diatoms. Mar. Biol. 103, 119–129.
[9] Ploug, H. et al. (1997) Anoxic aggregates – an ephemeral phenomenon in the ocean? Aquat. Microb. Ecol. 13, 285–294.
[10] Brzezinski, M.A., O'Bryan, L.M. and Alldredge, A.L. (1997) Silica cycling within marine snow. Limnol. Oceanogr. 42, 1706–1713.
[11] Bidle, K.D. and Azam, F. (2001) Bacterial control of silicon regeneration from diatom detritus: Significance of bacterial ectohydrolases and species identity. Limnol. Oceanogr. 46, 1606–1623.
[12] Schrader, H.J. (1972) Anlösung und Konservierung von Diatomeenschalen beim Absinken am Beispiel des Landsort-Tiefs in der Ostsee. Nova Hedwigia 39, 191–216.
[13] Takahashi, K. (1986) Seasonal fluxes of pelagic diatoms in the subarctic pacific 1982–1983. Deep-Sea Res. I 33, 1225–1251.
[14] Guillard, R.R.L. (1975) Culture of phytoplankton for feeding marine invertebrates. In: Culture of Marine Invertebrate Animals (Smith, W.L. and Chanley, M.H., Eds.), pp. 108–132. Plenum Press, New York.
[15] Shanks, A.L. and Edmondson, E.W. (1989) Laboratory-made artificial marine snow: A biological model of the real thing. Mar. Biol. 101, 463–470.
[16] Koroleff, F. (1983) Determination of nutrients. In: Methods of Seawater Analysis (Grasshoff, K., Erhardt, M. and Kremling, K., Eds.), pp. 125–187. Verlag Chemie, Weinheim.
[17] Parsons, T.R., Maita, Y. and Lalli, C.M. (1984) A Manual for Chemical and Biological Methods for Seawater Analysis. Pergamon Press, New York.
[18] Passow, U. and Alldredge, A.L. (1995) A dye-binding assay for the spectrophotometric measurement of transparent exopolymer particles (TEP). Limnol. Oceanogr. 40, 1326–1335.
[19] Passow, U. and Alldredge, A.L. (1994) Distribution, size, and bacterial colonization of transparent exopolymer particles (TEP) in the ocean. Mar. Ecol. Prog. Ser. 113, 185–198.
[20] Logan, B.E. and Alldredge, A.L. (1989) Potential for increased nutrient uptake by flocculating diatoms. Mar. Biol. 101, 443–450.
[21] Alldredge, A.L. and Gotschalk, C. (1988) In situ settling behavior of marine snow. Limnol. Oceanogr. 33, 339–351.
[22] Lick, W., Huang, H. and Jepson, R. (1993) Flocculation of fine-grained sediments due to differential settling. J. Geophys. Res. 98, 10279–10288.
[23] Logan, B.E. and Wilkinson, B.D. (1990) Fractal geometry of marine snow and other biological aggregates. Limnol. Oceanogr. 35, 130–135.
[24] Kilps, J.R., Logan, B.E. and Alldredge, A.L. (1994) Fractal dimensions of marine snow determined from image analysis of in situ photographs. Deep-Sea Res. 41, 1159–1169.
[25] Jiang, Q. and Logan, B.E. (1991) Fractal dimensions of aggregates determined from steady-state size distributions. Environ. Sci. Technol. 25, 2031–2038.
[26] Logan, B.E. and Kilps, J.R. (1995) Fractal dimensions of aggregates formed in different fluid mechanical environments. Water Res. 29, 443–453.
[27] Ploug, H. and Jorgensen, B.B. (1999) A net-jet flow system for mass transfer and microsensor studies of sinking aggregates. Mar. Ecol. Prog. Ser. 176, 1–38.
[28] Kiørboe, T., Ploug, H. and Thygesen, U.H. (2001) Fluid motion and solute distribution around sinking aggregates. I. Small-scale fluxes and heterogeneity of nutrients in the pelagic environment. Mar. Ecol. Prog. Ser. 211, 1–13.
[29] Logan, B.E. and Hunt, J.R. (1987) Advantages to microbes of growth in permeable aggregates in marine systems. Limnol. Oceanogr. 32, 1034–1048.
[30] Blank, G.S. and Sullivan, C.W. (1979) Diatom mineralization of silicic acid-III, $Si(OH)_4$ binding and light dependent transport in Nitzschia angularis. Arch. Microbiol. 123, 157–164.
[31] Cappellen, P.V. and Qui, L. (1997) Biogenic silica dissolution of the Southern Ocean: II Kinetics. Deep-Sea Res. II 44, 1129–1149.
[32] Greenwood, J.E., Truesdale, V.W. and Rendell, A.R. (2001) Biogenic silica dissolution in seawater – in vitro chemical kinetics. Prog. Oceanogr. 48, 1–23.
[33] Kiørboe, T. (2000) Colonization of marine snow aggregates by invertebrate zooplankton: Abundance, scaling, and possible role. Limnol. Oceanogr. 45, 479–484.
[34] Jackson, G.A. (1990) A model of the formation of marine algal flocks by physical coagulation processes. Deep-Sea Res. 37, 1197–1211.
[35] Dam, H.G. and Drapeau, D.T. (1995) Coagulation efficiency, organic-matter glues, and the dynamics of particles during a phytoplankton bloom in a mesocosm study. Deep-Sea Res. II 42, 111–123.
[36] Engel, A. (2000) The role of transparent exopolymer particles (TEP) in the increase in apparent particle stickiness (alpha) during the decline of a diatom bloom. J. Plankton Res. 22, 485–497.
[37] Clifford, J., Li, X. and Logan, B. (1996) Settling velocities of fractal aggregates. Environ. Sci. Technol. 30, 1911–1918.
[38] Li, X. and Logan, B.E. (1997) Collision frequencies of fractal aggregates with small particles by differential aggregation. Environ. Sci. Technol. 31, 1229–1236.
[39] Li, X. and Logan, B.E. (1997) Collision frequencies between fractal aggregates and small particles in a turbulently sheared fluid. Environ. Sci. Technol. 31, 1237–1242.
[40] Cowen, J.P. and Holloway, C.F. (1996) Structure and chemical analysis of marine aggregates: In situ macrophotography and laser confocal and electron microscopy. Mar. Biol. 126, 163–174.
[41] Holloway, C.F. and Cowen, J.P. (1997) Development of a scanning confocal laser microscopic technique to examine the structure and composition of marine snow. Limnol. Oceanogr. 42, 1340–1352.
[42] Alldredge, A.L., Passow, U. and Logan, B.E. (1993) The abundance and significance of a class of large, transparent organic particles in the ocean. Deep-Sea Res. I 40, 1131–1140.
[43] Passow, U., Alldredge, A.L. and Logan, B.E. (1994) The role of particulate carbohydrate exudates in the flocculation of diatom blooms. Deep-Sea Res. I 41, 335–357.
[44] Revsbech, N.P., Nielsen, L.P. and Ramsing, N.B. (1998) A novel microsensor for determination of apparent diffusivity in sediments. Limnol. Oceanogr. 43, 986–992.
[45] Wieland, A. et al. (2001) Fine-scale measurements of diffusivity in a microbial mat with nuclear magnetic resonance imaging. Limnol. Oceanogr. 46, 248–259.
[46] Honjo, S., Mahganini, S.J. and Cole, J.J. (1982) Sedimentation of biogenic matter in the deep ocean. Deep-Sea Res. 29, 609–625.
[47] da Costa DeMacho, E. (1993) Production, sedimentation and dissolution of biogenic silica in the northern North Atlantic. In: Marine Planktology. University of Kiel, Kiel.
[48] Brzezinski, M.A. and Nelson, D.M. (1995) The annual silica cycle in the Sargasso Sea near Bermuda. Deep-Sea Res. 42, 1215–1237.

Downloaded from https://academic.oup.com/femsec/article/46/3/247/520432 by Max-Planck-Institute Bremen user on 15 December 2020